Acta Crystallographica Section D
Biological Crystallography
ISSN 0907-4449

Analysis of the effect of microgravity on protein crystal quality: the case of a myoglobin triple mutant

Adriana E. Miele, Luca Federici,† Giuliano Sciara, Federica Draghi,‡ Maurizio Brunori* and Beatrice Vallone

Dipartimento di Scienze Biochimiche and CNR Istituto di Biologia e Patologia Molecolari, Universita di Roma 'La Sapienza', P.le A. Moro 5, 00185 Rome, Italy

† Present address: Department of Biochemistry, 10 Tennis Court Road, Cambridge, England.
‡ Present address: MRC–Dunn Nutritional Unit, Hills Road, Cambridge, England.

Correspondence e-mail: maurizio.brunori@uniroma1.it

Received 11 December 2002
Accepted 13 March 2003

PDB References: Mb-YQR, microgravity-grown crystal, ISS 6A, 1n9h; earth-grown crystal, ISS 6A, 1n9f; microgravity-grown crystal, ISS 8A, 1n9x; earth-grown crystal, ISS 8A, 1n9i; near-atomic resolution diffracting microgravity-grown crystal, ISS 8A, 1naz.

Crystals of the Met derivative of the sperm whale myoglobin triple mutant Mb-YQR [L(*B*10)Y, H(*E*7)Q and T(*E*10)R] were grown under microgravity conditions and on earth by vapour diffusion. A comparison of crystal quality after complete data collection and processing shows how microgravity-grown crystals diffract to better resolution and lead to considerably improved statistics for X-ray diffraction data compared with crystals grown on earth under the same conditions. The same set of experiments was reproduced on two different Spacelab missions (ISS 6A and ISS 8A) in 2001 and 2002. The structure of this mutant myoglobin, refined using data collected at ELETTRA (Trieste, Italy) from both kinds of crystals, shows that X-ray diffraction from microgravity-grown crystals leads to better defined electron-density maps as well as improved geometrical quality of the refined model. Improvement of the stereochemical parameters of a protein structure is fundamental to quantitative analysis of its function and dynamics and hence to thorough understanding of the molecular mechanisms of action.

1. Introduction

Myoglobin (Mb) has been employed as a model for investigating the complex relationships between structure and function in small globular proteins ever since its structure was determined (Kendrew *et al.*, 1960). Such studies took advantage of the rich optical spectrum of Mb upon binding of O_2 and other small ligands (Antonini & Brunori, 1971). The three-dimensional structure of Mb clearly shows that the haem prosthetic group is deeply buried inside the protein scaffold and that there is no obvious channel for the ligands to diffuse to and from the haem iron. In 1966, Perutz and Matthews proposed that a side-chain rotation of the distal His64(*E*7) of sperm whale Mb could be responsible for ligand migration to and from the solvent. This hypothesis was subsequently confirmed by structural studies on different myoglobins (Bolognesi *et al.*, 1982) and supported by extensive kinetic experiments on site-directed mutants (Scott *et al.*, 2001). The photosensitivity of the reduced protein bound to CO, NO and O_2 allows the migration of ligands through the protein matrix to be followed. Recent crystallographic experiments on reaction intermediates captured by nanosecond Laue crystallography (Srajer *et al.*, 2001; Bourgeois *et al.*, 2003) have shown that packing defects and internal cavities present in globular proteins play a role in controlling the diffusion of ligand/substrate to the active site, as has been suggested by others (Schlichting & Chu, 2000; Brunori & Gibson, 2001).

We have previously characterized a sperm whale Mb triple mutant Mb-YQR with the following substitutions: L(*B*10)Y,

H(*E*7)Q and T(*E*10)R (Travaglini-Allocatelli *et al.*, 1994). This mutant, originally designed to reproduce the unusually slow O_2-dissociation rate of *Ascaris suum* haemoglobin, proved interesting for assessing the functional role of packing defects and conformational substates. Different experimental approaches, ranging from crystal structure determination of the oxy and deoxy derivatives to laser photolysis and molecular-dynamics simulation (Brunori *et al.*, 2000; Draghi *et al.*, 2002; Lamb *et al.*, 2002), showed that the pathway of a small ligand in its trajectory through the protein can be modified by site-directed mutagenesis and that migration within the protein matrix to the active site involves a limited number of pre-existing cavities identified in the interior space of a protein through the binding of xenon (Tilton *et al.*, 1984).

Further work using time-resolved crystallography is necessary to obtain a better definition of the structural dynamics that controls the diffusion of ligands from the solvent to the active site through specific internal pathways. In this perspective, very high quality crystals that diffract to atomic resolution and are well ordered and fully homogeneous are in demand.

In the recent past we have seen considerable efforts to improve crystallization techniques and obtain higher diffraction-quality crystals. One promising approach has been to take advantage of space-shuttle missions to carry out crystallization experiments under microgravity conditions. The rationale for attempting such experiments is that microgravity should increase the physical perfection and volume of the crystals by the reduction of buoyancy and sedimentation effects (McPherson, 1993; Vekilov, 1999). In some cases this approach proved successful (Long *et al.*, 1994; Wardell *et al.*, 1997; Berisio *et al.*, 2002; Ng *et al.*, 2002) and experimental evidence obtained with various proteins provided a clue that the idea underlying microgravity crystallization may bear some truth.

Here, we report the first crystallographic microgravity experiments performed on a myoglobin, choosing a site-directed mutant. Mb-YQR was selected for this experiment not only for its peculiar functional properties, but also for its ease of yielding crystals, which belong to a high-symmetry space group and quite often show some defects or tend not to be single.

Two sets of crystals were grown in microgravity in two different space missions [namely International Space Station (ISS) 6A and ISS 8A] and were grown in parallel on earth under the same conditions. Crystals were tested for diffraction in the synchrotron beam source at ELETTRA (Trieste, Italy). Complete data collections were obtained from crystals belonging to both subsets. The structure of the oxidized derivative of Mb-YQR was determined using data obtained from the best crystal of each subset and protein models were compared. 1 y later we carried out the same set of experiments in a different space mission (ISS 8A) using a different purification batch of the protein, proving the high reproducibility of the methodology. We show below that microgravity crystals diffracted to a better resolution and that mosaicity as well as all statistical parameters of data processing were improved compared with earth-grown crystals. We also show that these higher quality data led to better defined electron-density maps and to a protein model with improved geometrical parameters.

2. Methods

2.1. Crystallization

Crystals of the oxidized derivative of Mb-YQR were grown using the vapour-diffusion method in the High Density Protein Crystal Growth System (HDPCG) apparatus during International Space Station flight 6A (ISS 6A, April–July 2001). Two synchronized sets of experiments were carried out in parallel in microgravity conditions and on earth for control. Mb-YQR, concentrated to 20 mg ml^{-1}, was mixed with an equal volume of three different reservoir solutions: 100 m*M* Tris–HCl pH 8.7, 1 m*M* EDTA and 2.7 *M* (reservoir 1), 2.8 *M* (reservoir 2) or 2.9 *M* (reservoir 3) ammonium sulfate. The total volume of the droplets was 10 µl and the reservoir volume was 560 µl. Protein samples and reservoir solutions were sent to NASA Laboratories (Centre for Biophysical Sciences and Engineering) and the HDPCG apparatuses for microgravity experiments were loaded before each launch. Both sets of experiments were activated by the crew once the apparatuses were transferred in the ISS and deactivated before moving them to the shuttle for returning to earth. The total number of HDPCG apparatuses used was four (one apparatus for reservoir 1, two for reservoir 2 and one for reservoir 3, each containing six reactors) and they were allocated into a Single-locker Thermal Enclosure System with a controlled temperature of 296 K. The same protocol was applied during the mission ISS 8A, which spanned April–June 2002. In this case, the HDPCG system has been siliconized prior to use and only one precipitant condition was tested (2.7 *M* ammonium sulfate, 100 m*M* Tris–HCl pH 8.7, 1 m*M* EDTA) with a total of 12 reactors. During mission ISS 6A crystals were allowed to grow for 83 d before deactivation, while during mission ISS 8A growth spanned 71 d.

2.2. Data collection and processing

All the experimental measurements of earth and microgravity crystals were performed at the XRD beamline (equipped with a MAR CCD detector) of the ELETTRA synchrotron (Trieste, Italy) on either 8 September 2001 or 12 July 2002. Measurements were performed at 100 K and 20% glycerol was used as cryoprotectant agent. In the first case, of all the crystals grown in microgravity a total of six were tested for diffraction, all of which were single; the best three were subjected to data collection. On the other hand, 12 crystals grown on earth under the same conditions were tested; only two proved to be single and suitable for data collection. At the end of the second mission, three crystals from microgravity were tested and two collected. Of these one was single and diffracted to 1.4 Å, while the other was not single but, given its nearly atomic resolution diffraction, data were collected anyway. As regards the earth-grown crystals, 11 were tested and the only two single crystals were used for data collection.

All data were processed with *DENZO* and scaled with *SCALEPACK* (Otwinowski & Minor, 1997). Intensities were converted to structure factors using the program *TRUNCATE* (French & Wilson, 1978; Collaborative Computational Project, Number 4, 1994) and a set of 5% of total reflections were selected by *FREERFLAG* (Brünger, 1992; Collaborative Computational Project, Number 4, 1994) for subsequent free *R*-factor analysis.

2.3. Structure solution and refinement

The coordinates of oxy Mb-YQR (PDB code 1f65; Brunori *et al.*, 1999), omitting the oxygen molecule, were used as an initial model to calculate difference Fourier maps ($2F_o - F_c$) with *FFT* (Read & Schierbeek, 1988; Collaborative Computational Project, Number 4, 1994). Structures were refined with the maximum-likelihood algorithm as implemented in *REFMAC* (Murshudov *et al.*, 1997). *B* factors were refined isotropically for all the structures except the nearly atomic resolution structure, where they were refined anisotropically. After each cycle of refinement, $2F_o - F_c$ and $F_o - F_c$ maps were calculated and visualized with *QUANTA* (MSI Inc., CA, USA) to manually adjust the model in the experimental electron density. Water molecules were added using the X-Solvate module of the *QUANTA* package. The final model's geometrical quality was validated using *PROCHECK* (Laskowski *et al.*, 1998; Collaborative Computational Project, Number 4, 1994).

3. Results

Freshly prepared Mb-YQR protein samples were grown in microgravity on two different International Space Station missions, namely ISS 6A (April–July 2001) and ISS 8A (April–June 2002), within the framework of the NASA Microgravity Crystal Growth Program.

3.1. Pre-flight experiments

Crystals of different derivatives of Mb-YQR were previously obtained in our laboratory by the hanging-drop vapour-diffusion method using conventional Linbro plates and siliconized cover slips. We used this information as a starting point for obtaining suitable crystals with the HDPCG apparatus in a time window compatible with the scheduled length of the ISS missions. The previously determined conditions produced crystals in three weeks to one month; an effort was therefore made to optimize the precipitant concentration to allow faster growth in the new setup. In fact, by increasing the precipitant concentration Mb-YQR crystals obtained on earth appeared after 6 d and reached their final dimensions in 10 d.

Table 1
Data collection and processing.

Values in parentheses refer to the last resolution shell.

	ISS 6A		ISS 8A	
	Microgravity (1n9h)	Earth (1n9f)	Microgravity (1n9x)	Earth (1n9i)
Resolution range (Å)	15.0–1.5 (1.52–1.50)	15–1.8 (1.83–1.80)	20.0–1.4 (1.48–1.4)	20.0–1.6 (1.69–1.60)
Space group	*P*6	*P*6	*P*6	*P*6
Unit-cell parameters (Å)				
a, *b*	90.580	90.542	90.277	90.37
c	45.254	45.242	45.185	45.175
Mosaicity (°)	0.33	0.71	0.24	0.38
No. unique reflections	31153	21977	39786	27908
No. rejected reflections	295	4341	1057	3576
Average $I/\sigma(I)$	13.4	15.6	49.1	29.3
Completeness (%)	98.3 (96.7)	98.5 (86.7)	99.9 (100)	99.9 (100
χ^2 (overall)	0.781	1.242	1.012	1.232
$R_{\rm merge}$	0.045 (0.320)	0.089 (0.207)	0.025 (0.048)	0.033 (0.129)
Isotropic mean *B* factor from Wilson plot (Å^2)	12.29	18.51	11.29	14.58

3.2. Post-flight ISS 6A experiments

Inspection of the crystallization reactors after landing revealed the presence of crystals in all of them. Crystals appeared well developed in all dimensions and grew up to 100 × 100 × 50 µm. On the other hand, crystals were only present in a few reactors of the on-earth experiments; they tended to grow in multilayer disordered rose-like shapes.

A comparative analysis of crystal quality was performed by measuring the diffraction pattern of numerous microgravity-grown and earth-grown crystals at ELETTRA. Initially, the same exposure dose, oscillation range and crystal-to-detector distance were applied to both microgravity-grown and earth-grown crystals; however, clear differences within the two sets of crystals were detected, all microgravity-grown crystals yielding better resolution. To give a statistical relevance to these first observations, six crystals from the microgravity-grown and 12 from the earth-grown subsets were tested. Complete data collection was performed with three microgravity-grown crystals and with the two single crystals from the earth-grown subset. In these data collections, the crystal-to-detector distance was adjusted to the effective resolution limits and the same number of exposures and oscillation degree were used throughout. Microgravity-grown crystals appeared to diffract to higher resolution and complete data to 1.5 Å resolution could be measured; in contrast, crystals grown on earth revealed a resolution limit of 1.8 Å.

In Table 1 the relevant statistical parameters of data processing and scaling of the best crystal of each subset are shown. Major improvements were detected with respect to all the statistical parameters, *i.e.* mosaicity (as determined by *SCALEPACK*), overall completeness and completeness in the highest resolution shell, $R_{\rm merge}$ and χ^2. In Fig. 1 the overall diffraction patterns of the two crystals are shown together with an enlargement of the edge-of-frame region. A large anisotropy is apparent in the crystal grown on earth that cannot be detected in that grown in microgravity.

3.3. Post-flight ISS 8A experiments

1 y later the same set of experiments was repeated, introducing a modification in the moulded polysulfone HDPCG apparatus. We had noticed that the crystals grew attached to the walls of the cells and it had been hard to extract them with anything but a Pasteur pipette. Since this handling could cause damage, we decided to siliconize the HDPCG apparatus. This proved very successful and we could gently fish out the crystals with a mounting loop from both sets of reactors.

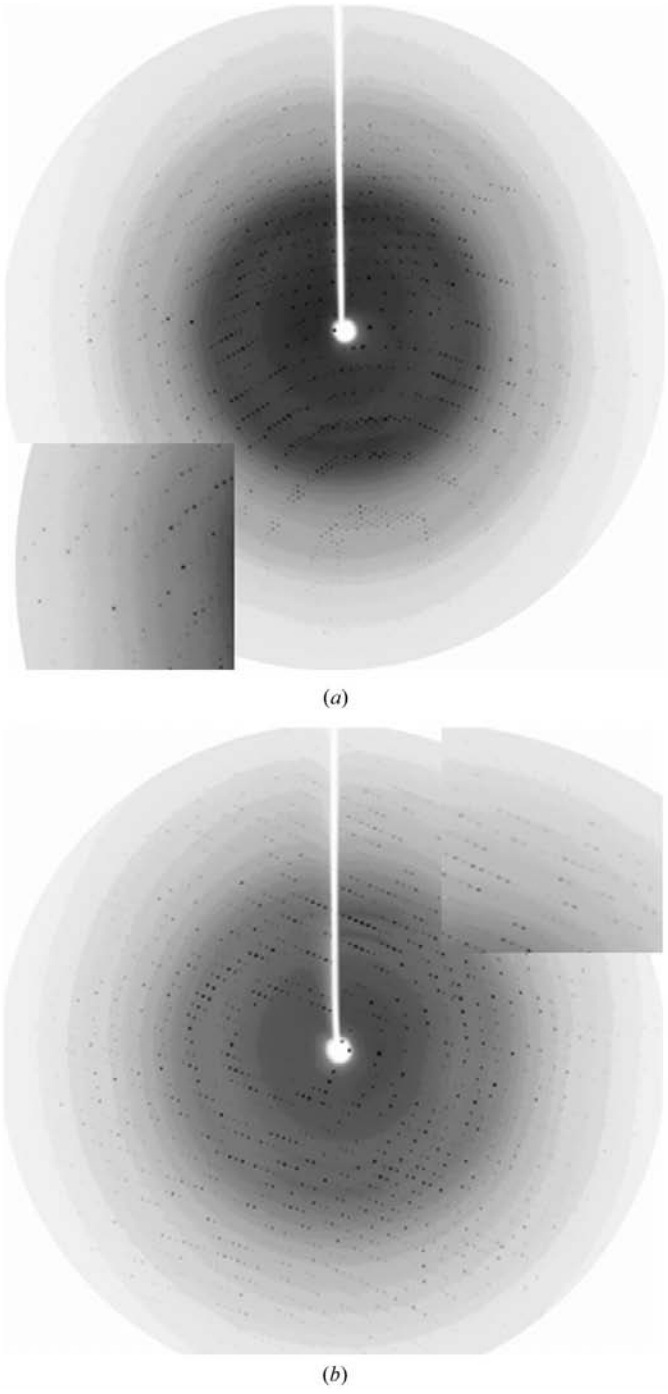

Figure 1
An example of the diffraction pattern of the best crystal of Mb-YQR grown in microgravity (*a*) and on earth (*b*). The inset in each panel depicts a magnification of the edge of the frame.

Table 2
Results of refinement of the structures of oxidized Mb-YQR.

	ISS 6A		ISS 8A	
	Microgravity (1n9h)	Earth (1n9f)	Microgravity (1n9x)	Earth (1n9i)
Resolution range (Å)	15.0–1.8	15.0–1.8	20.0–1.6	20.0–1.6
R_{cryst} (%)	15.4	17.9	17.7	18.8
Free R_{cryst}† (%)	15.9	20.2	20.0	20.1
FOM	0.893	0.877	0.898	0.883
R.m.s. deviations				
Bond lengths (Å)	0.010	0.014	0.0044	0.0062
Bond angles (°)	1.01	1.89	0.8005	0.879
Total No. of atoms	1384	1329	1512	1413
No. of water molecules	171	97	227	158
Mean isotropic *B* factor from *BAVERAGE* (Å^2)	14.32	21.96	10.72	11.69

Hence, we reassuringly confirmed the ISS 6A result and improved it. In fact, earth-grown crystals were fewer and mostly multilayered, while the microgravity-grown ones were mostly single-shaped and larger (up to 180 × 180 × 80 µm compared with 140 × 140 × 40 µm for the largest earth-grown crystal). A comparative analysis was carried out in the same way as for the previous experiment and two complete data sets per batch were measured: namely, onr microgravity-grown crystal at 1.4 and at 1.04 Å; one earth-grown crystal at 1.85 and one at 1.6 Å.

The near-atomic resolution diffracting crystal was not single; however, the main lattice was so intense and neat as to allow very satisfactory processing of the data. Nevertheless, for our comparative purposes we decided to use the single crystal diffracting at 1.4 Å in order not to be biased by intrinsic crystal imperfections. For example, the value of the mosaicity calculated in a non-single crystal could be overestimated and thus may be statistically non-significant. The near-atomic structure at 1.04 Å was solved and the resulting model compared with the other two sets.

3.4. Structure determination and refinement

In order to assess how much the overall quality of crystals and of experimental data collection is reflected in the quality of the electron-density maps and in the geometrical parameters of the final model, we solved and refined the structure of the oxidized derivative of Mb-YQR from the subsets of earth-grown and microgravity-grown crystals. For comparative purposes, the same resolution ranges and refinement protocols have been used, *e.g.* 1.8 Å for data from ISS 6A and 1.6 Å for data from ISS 8A. The refinement statistics are reported in Table 2. In Fig. 2, the electron-density maps of a critical area of the Mb, the haem pocket, are shown for the two models of ISS 6A. The maps of microgravity-grown crystals appear better defined, especially in the residuals. This result may be a direct consequence of a more ordered packing of the molecules within the *P*6 lattice, reflecting a mosaicity value that is

almost halved with respect to the earth-grown crystal as judged by *SCALEPACK*. Not unexpectedly, the overall structure of the two models is superimposable. The averaged root-mean-square deviation calculated with the MODELER module of program *QUANTA* (Molecular Structure Inc., CA, USA) is respectively 0.49 Å for the main-chain atoms and 0.85 Å including all the side-chain atoms for data from ISS 6A and 0.23 Å for the main-chain atoms and 0.90 Å including all the side-chain atoms for data from the ISS 8A experiment. The main difference lies in the better value of r.m.s.d. for main-chain atoms obtained in the ISS 8A set with respect to the ISS 6A set. This result could be a consequence of the higher resolution of the data used to refine the models (1.6 compared with 1.8 Å) as well as the higher quality of crystals grown in the second mission (see Table 1), which is possibly related to the gentler handling of crystals that was allowed by the siliconization procedure.

Furthermore, looking at the overall *B* factor (which has deliberately been refined as isotropic in all cases), it is apparent how the errors can accumulate in this number, which also represents the estimated accuracy of a model. Moreover, the main difference between the model from ISS 6A and ISS 8A lies in the conformation of E7Q, which was apparently double in the first case, while definitely single and corresponding to the conformer closer to B10Y in the latter case (both in the earth model and in the two microgravity models).

Differences between the structure of the oxidized and oxygenated derivative of Mb-YQR unsurprisingly mainly lay in the haem pocket. On the distal side a density for an O atom has been refined. Given the basic pH of crystallization (8.7) and supported by the spectrum taken after dissolving the crystal, we assumed that the atom was indeed a mixed population of H_2O and OH^- bound to the iron; unfortunately, the near-atomic resolution of 1.04 Å is not high enough to show H atoms and hence we have not been able to discriminate between or calculate the respective percentage of the populations.

A distinctive network of hydrogen bonds marks the structure and that which can only be inferred from the data at lower resolution is shown to be correct by inspecting the electron-density map at 1.04 Å.

3.5. Near-atomic resolution structure of Mb-YQR at 1.04 Å.

The space mission ISS 8A proved particularly successful, leading to the growth of a crystal diffracting to near-atomic resolution. However, as already stated above, owing to the presence of a weak second lattice the model refined at this resolution was not used for statistical comparison. In this case, the same starting model (PDB code 1f65) was used as a search model, giving rise to the values reported in Table 3. Owing to the very high resolution, we could assign double conformations to 34 amino-acid side chains. Even the N- and C-termini are better defined and in some cases extra density attributable to H atoms is visible. The number of water molecules has doubled, approaching the quantity of solvent predicted by the Matthews coefficient.

In the haem pocket, the proximal His—Fe bond (not constrained during refinement) achieved a value of 2.062 Å, while the Fe—O bond is 2.016 Å (Fig. 3). These values are in excellent agreement with the values independently obtained by solution experiments reported in the literature (Perutz, 1979; Chance *et al.*, 1996). Furthermore, this model allowed us to measure the hydrogen-bonding network in the haem pocket with high accuracy: Tyr*B*10—Gln*E*7 is 2.673 Å, Gln*E*7—O is 3.174 Å and Tyr*B*10—O is 2.916 Å.

A root-mean-square deviation between the model at atomic resolution and that from ISS 8A used for comparison (the

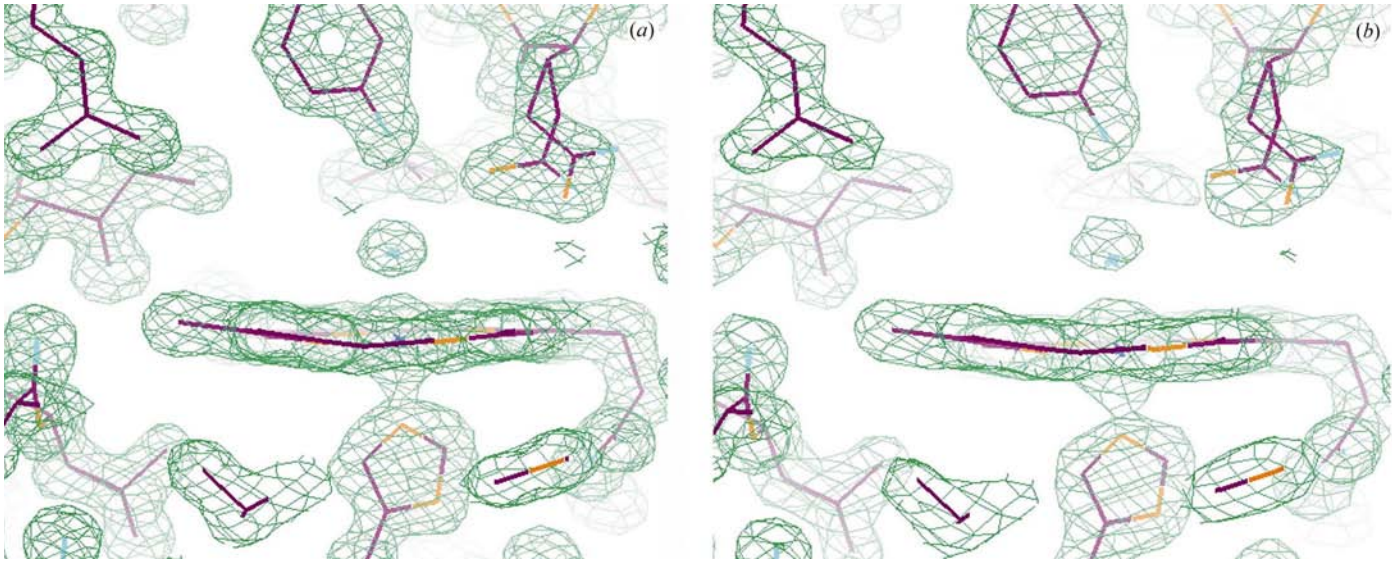

Figure 2
Model of oxidized Mb-YQR refined from microgravity-grown crystals form the ISS 6A mission (*a*) and earth-grown crystals (*b*) as a control. A close up of residues lining the haem pocket is presented. In each panel a $2F_o - F_c$ map (magenta) contoured at 1σ is shown.

Table 3
Crystallographic parameters for Mb-YQR at nearly atomic resolution (PDB code 1naz).

Values in parentheses are for the last resolution shell.

Data collection and processing	
Resolution range (Å)	20.0–1.04 (1.07–1.04)
Space group	*P*6
Unit-cell parameters (Å)	
a, *b*	90.06
c	45.17
Mosaicity (°)	0.32
No. of unique reflections	97313
No. of rejected reflections	1073
Average $I/\sigma(I)$	22.4
Completeness (%)	99.8 (100)
χ^2 (overall)	1.010
$R_{\rm merge}$ (overall)	0.030 (0.154)
Isotropic mean *B* factor from Wilson plot (Å^2)	8.874
Refinement statistics	
$R_{\rm cryst}$ (%)	13.20
Free $R_{\rm cryst}$ (%)	14.65
FOM	0.943
R.m.s. deviation	0.0039
Bond lengths (Å)	0.0039
Bond angles (°)	0.701
Total No. of atoms	1664
Total No. of water molecules	339
Mean isotropic *B* factor from *BAVERAGE* (Å^2)	9.541

resolution of which was 1.4 Å) has been calculated, giving a difference of 0.09 Å for the main chain and an overall difference of 0.59, mainly arising from the difference in the number of residues with a double conformation. This very good agreement between the high-resolution structures confirms the need for good quality of the raw data in order to achieve the best results.

4. Discussion

In this paper, we present the structure of the oxidized derivative of a site-directed mutant of sperm whale myoglobin carrying the following mutations: L(*B*10)Y, H(*E*7)Q and T(*E*10)R (Mb-YQR). The structure was solved by means of X-ray diffraction on single crystals grown under microgravity conditions on two different International Space Station missions, namely ISS 6A (April–August 2001) and ISS 8A (April–June 2002). The three-dimensional structures from space have been compared with those obtained from crystals grown on earth in parallel under exactly the same conditions. Mb-YQR has been extensively studied and the three-dimensional structures of its deoxy, oxy and CO derivatives have been published (Brunori *et al.*, 1999). The ultimate goal of structural biologists is to understand the function of a protein, interpreting solution studies in atomic terms and trying to generalize the subsequent results to a broader range. In order to quantify the relationships between structure and function, not only does the wet biology have to be very accurate, but the model of the three-dimensional structure of interest has to be as close to reality as possible; hence the importance of atomic resolution in crystallography and the consequent need for a very homogeneous and extremely ordered crystal packing, since imperfections can propagate and affect the final model. Unfortunately, ideality is far from being achieved in such an empirical art as protein crystallization, but efforts have been made to control possible parameters.

Several groups have shown (Snell *et al.*, 1997; Borgstahl *et al.*, 2001) that molecules which pack themselves in high symmetry space groups (*P*4 and higher) need more effort in order to generate large and well diffracting species. The quasi-absence of convection and sedimentation obtainable in microgravity helps to improve the shape of these crystals because it can counterbalance the different velocity of nucleation in the three dimensions. Molecules will have a higher probability of being incorporated at a uniform rate, favouring isotropic growth (Kundrot *et al.*, 2001; Vergara *et al.*, 2003).

In this work, we have tested the vapour-diffusion technique for crystal growth in the High Density Protein Crystal Growth (HDPCG) apparatus, kindly provided by NASA. The results obtained in the first mission allowed us to further improve the diffraction quality of crystals in the second mission. In particular, only the crystal-growth condition which gave rise to the best diffracting crystals of the first mission was selected in the second one. Moreover, to overcome the tendency of these crystals to attach to the moulded polysulfone wells of the HDPCG, we decided to siliconize the apparatus prior to use. This procedure proved very successful, enabling us to minimize the imperfections arising from post-growth handling. Hence, we recommend that siliconization is used routinely whenever crystals tend to grow attached to the support.

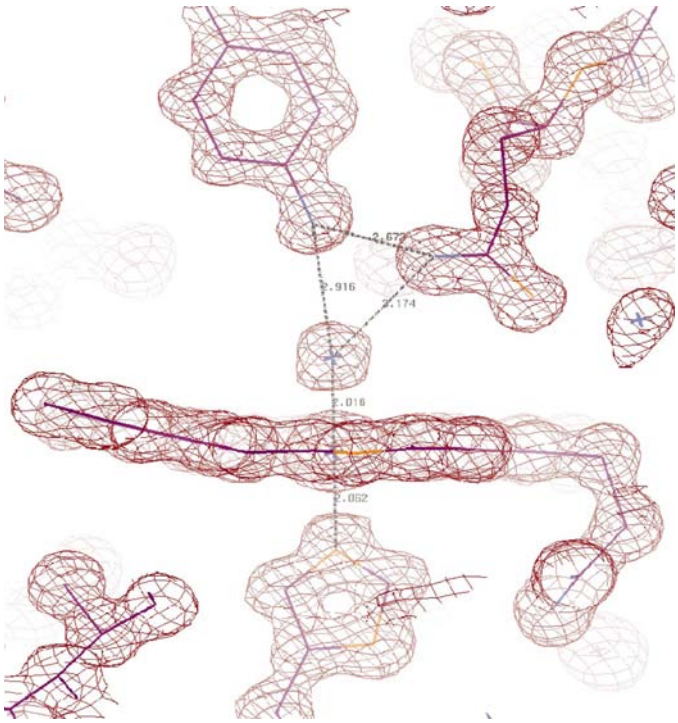

Figure 3
Close up of the haem pocket Mb-YQR at 1.04 Å from the ISS 8A mission. The hydrogen-bond network in the distal pocket and the iron distances to the 5th and 6th coordination positions are highlighted.

The improvement in the quality of Mb-YQR microgravity-grown crystals is impressive. Not only did the crystals diffract X-rays more intensely and to higher resolution, but they also displayed considerably reduced mosaicity values (by up to 50%). The latter feature is of crucial importance whenever a time-resolved crystallography experiment is to be attempted (Srajer *et al.*, 2001; Bourgeois *et al.*, 2003). The high-quality data of the space-grown crystals allowed us to build a very accurate model of the structure of the oxidized derivative of the mutant Mb-YQR. Moreover, crystals obtained in microgravity will be further manipulated in the near future in order to obtain a CO derivative suitable for time-resolved Laue diffraction. Such experiments may allow us to follow the ligands in their pathway in and out the protein matrix, quantitatively estimating the relative time courses and the role of structural dynamics (evaluated at near-atomic resolution) in controlling protein function.

We gratefully acknowledge the crews of the two Space Station Missions ISS 6A and ISS 8A for activating and deactivating the experiments on the Spacelab, the crews of the Space Shuttle missions STS-100, STS-105, STS-110 and STS-111 for orbiting and deorbiting the apparatus, and Dr Karen Moore and the staff at the Center for Biophysical Sciences and Engineering of NASA for providing the apparatus for microgravity crystal growth and for loading the sample prior to launch. We would like to thank Dr Alberto Cassetta of ELETTRA Synchrotron in Trieste for beam-time allocation and data collection. This work was supported by grants from the Agenzia Spaziale Italiana (Network for Crystallization in Space).

References

Antonini, E. & Brunori, M. (1971). *Hemoglobin and Myoglobin in their Reactions with Ligands.* Amsterdam: North Holland.
Berisio, R., Vitagliano, L., Mazzarella, L. & Zagari, A. (2002). *Protein Sci.* **11**, 262–270.
Bolognesi, M., Cannillo, E., Ascenzi, P., Giacometti, G. M., Merli, A. & Brunori, M. (1982). *J. Mol. Biol.* **158**, 305–315.
Borgstahl, G. E., Vahedi-Faridi, A., Lovelace, J., Bellamy, H. D. & Snell, E. H. (2001). *Acta Cryst.* D**57**, 1204–1207.
Bourgeois, D., Vallone, B., Schotte, F., Arcovito, A., Miele, A. E., Sciara, G., Wulff, M., Anfinrud, P. & Brunori, M. (2003). Submitted.
Brünger, A. T. (1992). *Nature (London)*, **355**, 472–474.
Brunori, M., Cutruzzola, F., Savino, C., Travaglini-Allocatelli, C., Vallone, B. & Gibson, Q. H. (1999). *Biophys. J.* **76**, 1259–1269.
Brunori, M., Vallone, B., Cutruzzola, F., Travaglini-Allocatelli, C., Berendzen, J., Chu, K., Sweet, R. M., & Schlichting, I. (2000). *Proc. Natl Acad. Sci. USA*, **97**, 2058–2063.
Brunori, M. & Gibson, Q. H. (2001). *EMBO Rep.* **2**, 674–679.
Chance, M. R., Miller, L. M., Fischetti, R. F., Scheuring, E., Huang, W. X., Sclavi, B., Hai, Y. & Sullivan, M. (1996). *Biochemistry*, **35**, 9014–9023.
>Collaborative Computational Project, Number 4 (1994). *Acta Cryst.* D**50**, 760–763.
Draghi, F., Miele, A. E., Travaglini-Allocatelli, C., Vallone, B., Brunori, M., Gibson, Q. H. & Olson, J. S. (2002). *J. Biol. Chem.* **277**, 7509–7519.
French, G. S. & Wilson, K. S. (1978). *Acta Cryst.* A**34**, 517.
Kendrew, J. C., Dickerson, R. E., Strandberg, B. E., Hart, R. G., Davis, D. D., Phillips, D. C. & Shore, V. C. (1960). *Nature (London)*, **185**, 422–427.
Kundrot, C. E., Judge, R. A., Pusey, M. L. & Snell, E. H. (2001). *Cryst. Growth Des.* **1**, 87–99.
Lamb, D. C., Nienhaus, K., Arcovito, A., Draghi, F., Miele, A. E., Brunori, M. & Nienhaus, G. U. (2002). *J. Biol. Chem.* **277**, 11636–11644.
Laskowski, R. A., Moss, D. S. & Thornton, J. M. (1998). *J. Mol. Biol.* **231**, 1049–1067.
Long, M. M., DeLucas, L. J., Smith, C., Carson, M., Moore, K., Harrington, M. D., Pillion, D. J., Bishop, S. P., Rosenblum, W. M., Naumann, R. J., Chait, A., Prahl, J. & Bugg, C. E. (1994). *Microgravity Sci. Technol.* **7**, 196–202.
McPherson, A. (1993). *Microgravity Sci. Technol.* **6**, 101–109.
Murshudov, G. N., Vagin, A. A. & Dodson, E. J. (1997). *Acta Cryst.* D**53**, 240–255.
Ng, J. D., Sauter, C., Lorber, B., Kirkland, N., Arnez, J. & Giegé, R. (2002). *Acta Cryst.* D**58**, 645–652.
Otwinowski, Z. & Minor, W. (1997). *Methods Enzymol.* **276**, 307–326.
Perutz, M. F. (1979). *Annu. Rev. Biochem.* **48**, 327–386.
Read, R. J. & Schierbeek, A. J. (1988). *J. Appl. Cryst.* **21**, 490–495.
Schlichting, I. & Chu, K. (2000). *Curr. Opin. Struct. Biol.* **10**, 744–752.
Scott, E. E., Gibson, Q. H. & Olson, J. S. (2001). *J. Biol. Chem.* **276**, 5177–5188.
Snell, E. H., Cassetta, A., Helliwell, J. R., Boggon, T. J., Chayen, N. E., Weckert, E., Holzer, K., Schroer, K., Gordon, E. J. & Zakalsky, P. F. (1997). *Acta Cryst.* D**53**, 231–239.
Srajer, V., Ren, Z., Teng, T. Y., Schmidt, M., Ursby, T., Bourgeois, D., Pradervand, C., Schildkamp, W., Wulff, M. & Moffat, K. (2001). *Biochemistry*, **40**, 13802–13815.
Tilton, R. F. Jr, Kuntz, I. D. Jr & Petsko, G. A. (1984). *Biochemistry*, **23**, 2849–2857.
Travaglini-Allocatelli, C., Cutruzzolà, F., Brancaccio, A., Vallone, B. & Brunori, M. (1994). *FEBS Lett.* **352**, 63–66.
Vekilov, P. G. (1999). *Adv. Space Res.* **24**, 1231–1240.
Vergara, A., Lorber, B., Zagari, A. & Giegé, R. (2003). *Acta Cryst.* D**59**, 2–15.
Wardell, M. R., Skinner, R., Carter, D. C., Twigg, P. D. & Abrahams, J. P. (1997). *Acta Cryst.* D**53**, 622–625.